Geospatial Health 3(1), 2008, pp. 69-79

Mapping of zones potentially occupied by *Aedes vexans* and *Culex poicilipes* mosquitoes, the main vectors of Rift Valley fever in Senegal

Yves M. Tourre[1,2], Jean-Pierre Lacaux[3], Cecile Vignolles[4], Jacques-André Ndione[5,6], Murielle Lafaye[7]

[1]METEO-France, Toulouse, France; [2]LDEO of Columbia University, Palisades, USA; [3]OMP, Université Paul Sabatier (UPS), Toulouse, France; [4]MEDIAS-France, Toulouse, France; [5]Centre de Suivi Ecologique (CSE), Dakar, Sénégal; [6]LPAO-SF (ESP/UCAD), Dakar, Sénégal; [7]CNES, Toulouse, France

Abstract. A necessary condition for Rift Valley fever (RVF) emergence is the presence of *Aedes (Aedimorphus) vexans* and *Culex (Culex) poicilipes* mosquitoes carrying the arbovirus and responsible for the infection. This paper presents a detailed mapping in the Sahelian region of Senegal of zones potentially occupied by these mosquitoes (ZPOMs) whose population density is directly linked to ecozones in the vicinity of small ponds. The vectors habitats and breeding sites have been characterized through an integrated approach combining remote sensing technology, geographical information systems, geographical positioning systems and field observations for proper geo-referencing. From five SPOT-5 images (~10 m spatial resolution) with appropriate channels, a meridional composite transect of 290 x 60 km was first constructed at the height of the summer monsoon. Subsequent ZPOMs covered major ecozones from north to south with different hydrological environments and different patterns pond distributions. It was found that an overall area of 12,817 ha ± 10% (about 0.8% of the transect) is occupied by ponds with an average ZPOM 17 times larger than this (212,813 ha ± 10% or about 14% of the transect). By comparing the very humid year of 2003 with 2006 which had just below normal rainfall, the ZPOMs inter-annual variability was analyzed in a sandy-clayey ecozone with an important hydrofossil riverbed within the Ferlo region of Senegal. Very probably contributing to an increased abundance of vectors by the end of August 2003, it was shown that the aggregate pond area was already about 22 times larger than in August 2006, corresponding to an approximately five times larger total ZPOM. The results show the importance of pin-pointing small ponds (sizes down to 0.1 ha) and their geographical distribution in order to assess animal exposure to the RVF vectors.

Keywords: Rift Valley fever, arbovirus, ponds, high resolution remote sensing, zones potentially occupied by mosquitoes, Senegal.

Introduction

Higher than average seasonal amount of rainfall in East Africa lead to a seasonal increase of vector-borne epidemics, such as Rift Valley fever (RVF) (Linthicum et al., 1999) and malaria (Thomson et al., 2006). In Senegal and southern Mauritania, endemic malaria has been the main cause of morbidity and mortality, particularly during the half-of-the-year flooded valley of the Senegal river which is densely populated between Podor and Kaedi. With a rapidly increasing and migrating population and seasonal livestock movements, new epidemics occur in new areas. For example, with the appearance of the virus-carrying vectors *Aedes* (*Aedimorphus*) *vexans* Meigen and *Culex poicilipes* Theobald (Diptera: Culicidae) (Fontenille et al., 1998; Chevalier et al., 2005; Diallo et al., 2005), the Ferlo region south of the Senegal River became

Corresponding author:
Yves M. Tourre
METEO-France
DCLIM, 42, avenue Gaspard Coriolis
31057 Toulouse Cedex 01, France
Tel. +33 05 6107 8149; Fax +33 05 6107 8147
E-mail: yves.tourre@meteo.fr

quite rapidly a RVF-prone area during the late 1980s. As already shown by Ndione et al. (2003) and Lacaux et al. (2007), discrete and intense rainfall events (such as squall-lines with 20 mm of rainfall and more) appear to be the confounding parameter for RVF mosquito abundance (Mondet et al., 2005a,b). Modeling results by Porphyre et al. (2005) and Ndiaye et al. (2006), linking discrete rainfall events with pond dynamics and mosquito abundance/aggressiveness, have been successfully corroborated.

In a climate change context, population dynamics, and new eco-climatic conditions remain an on-going challenge for the prevention of epidemics (Pinzon et al., 2005). For example, the spatio-temporal distribution of rainfall governs the proliferation of RVF vectors near temporary ponds, which are the main watering sources for cattle and ruminants. It has been found that discrete rainy events, occurring less than seven days apart, may dramatically disturb *Ae. vexans* egg embryogenesis (Mondet et al., 2005a). Near these ponds/watering holes, vectors can easily transmit the virus to livestock (which then become domestic reservoirs) resulting in spontaneous abortions and prenatal mortality associated with huge local and regional socio-economic impact. Human RVF symptoms in Senegal are often limited to flu-like syndromes but could include more severe forms of encephalitis and hemorrhagic fever (Meegan and Bailey, 1988; Wilson et al. 1994).

In Senegal, the last decade has seen an increasing risk for RVF, both for animals and humans, which has resulted in a call for improving the early warning system (EWS) (Ndione et al., 2003; Mondet et al., 2005a,b). The French Spatial Agency (Centre National d'Etudes Spatiales, CNES) has been developing new multidisciplinary studies based on remote sensing (RS) technology to link climate-environment variability and potential re-emerging diseases. The goal with regard to the RVF vectors is to first use operational and high-spatial resolution RS images/data to detect all ponds (including their levels of turbidity with and without vegetation) for potential mosquito presence and breeding sites. A second aim is to map zones potentially occupied by mosquitoes (ZPOMs) in the vicinity of the Barkedji village, a testing site in the Ferlo region of Senegal. This was accomplished by developing novel indices derived from SPOT-5 images using the mean infrared (MIR) and the green and red channels, i.e. the normalized difference pond index (NDPI), which permits pond detection, and the normalized difference turbidity index (NDTI), which estimates pond turbidity as a measure of vector behaviour (Lacaux et al., 2007). Of note, the MIR data used ware not available from GeoEye and QuickBird high-spatial resolution products. The "classic" normalized difference vegetation index (NDVI) permitted the assessment of the vegetation cover within the ponds such as wild rice, water-lilies, etc. This technology made it possible to locate also small ponds with accuracy. The resulting ZPOM was obtained from entomological field-studies (Bâ et al., 2005) and mapped using flying ranges and spatial distribution of *Ae. vexans* and *Cx. poicilipes,* which thrive during the summer monsoon.

We have applied the technique to a much larger area than the Barkedji site, i.e. the whole Sahel region of Senegal, a meridional transect which covers four major ecological zones (ecozones) with different pond distributions which stretches from the Senegal river valley in the northeast to the Kaolack village in the south. It was constructed by using five high-resolution SPOT-5 images, again with appropriate infrared channels such as MIR and near infrared (NIR). The major ecozones display various orography (land elevations), rainfall regimes, hydrography and drainage which can be vertically ascending (Aranyossy et al., 2006). The substructure aquifers vary from hydromorphic soils, to the "sandy Ferlo" with intense wind erosion and poor water-retention capacity. It is expected that each ecozone responds differently to local rainy events which translates into differences in pond formation and their spatial distribution as well as ZPOMs uncertainties (from photo-interpretation and associated thresholds). It is acknowledged that, independently of the presence of ponds, the exposure of

livestock to RVF vectors has been accentuated by the numerous human-made boreholes, along the natural paths of nomadic population (Projet auto-promotion pastorale dans le Ferlo - PAPF - http://www.environnement.gouv.sn/article.php3?id_article=22).

Materials and methods

The conceptual approach of the present work (CNES, 2008) is much improved compared to the tools and techniques presented in Lacaux et al. (2007) and includes thresholds and associated ZPOMs uncertainties at seasonal and inter-annual timescales. Additional information is accessible through the RedGems website (http://www.redgems.org), a multi-disciplinary information system on climate, environment and epidemics.

Five SPOT-5 multi-spectral, high-resolution and re-processed "Level 2A" images (10 m for 17 August 2006) were assembled to form a meridional composite transect (~ 290 x 60 km = 17,400 km^2) in the Sahel, Senegal. The coordinates of the transect corners were: 16° 50' 44" N and 14° 46' 34" W; 16° 43' 35" N and 14° 13' 48" W; 14° 18' 52" N and 15° 21' 53" W; 14° 11' 46" N and 14° 49' 31" W (see the slanted rectangle in Fig. 2). The cloud coverage was discriminated using appropriate and digitalized masks.

ENVI software, version 4.3 (ITT Visual Solutions, http://www.ittvis.com) was used for image-processing. Image registration tools were used to warp and match images resulting in relative geo-referencing and minimized spatial errors. The methodology for detecting and classifying ponds as a function of turbidity and vegetation invasion was reminiscent to that described by Lacaux et al. (2007) and first applied to each single image (with their own NDPI, NDTI and NDVI) before compositing. It should be noted that the NDPI differs from the shortwave infrared (SWIR) index - based upon short-wavelength absorption by water and NIR, as used by Yi et al. (2007) - since it discriminates between actual small water bodies and/or humid soil and vegetation cover. The normalized difference water index (NDWI) (using NIR and MIR as described by Gao, 1996) was mainly used for vegetation water content estimates. A modified NDWI using the NIR and green channels enhanced the open-water features (McFeeters, 1996). Recently, a modified NDWI (replacing NIR by MIR from Landsat TM band 5) has been used by Xu (2006). The NDPI is from high-resolution SPOT-5 imagery. In addition, the high-resolution NDTI was used to detect water quality in terms of amount of suspended material, which affects mosquito behaviour (Paaijmans et al., 2008). In-situ observations by partners from the "Centre de Suivi Ecologique" (CSE/Dakar) validated the localization of given ponds using global positioning system (GPS) and geographical information system (GIS).

Based on the technologies mentioned above and by compositing the five images with their respective indices, it was possible to locate small ponds (down to 0.1 ha) for the full transect and to produce, for the first time, a composite ZPOM map. Pond mapping was produced through manual photo-interpretation and investigation of in-situ photographs for several and specific water bodies. Based on the above technique, two NDPI thresholds were identified. Each image was sorted twice according to the identified thresholds (Fig. 1) to obtain minimum and maximum pond areas.

From the pond mapping, the extremes are obtained, i.e. a minimum pond area (*Amin*) and a maximum pond area (*Amax*). "Mosaicking" and overlays from the five *Amin* (or *Amax*) maps led to two unique extremes maps for the transect. The derived statistics are obtained as follows:

$$Amean = (Amin + Amax)/2$$
$$\sigma = (((Amax - Amin)/2)/ Amean)*100$$
$$\boldsymbol{A} = Amean \pm \sigma$$

where *Amean* is the mean pond area and σ (in %) the associated uncertainties and ***A*** stands for pond areas with uncertainties.

From the ponds' extremes maps, associated ZPOMs were mapped (validated at the Barkedji

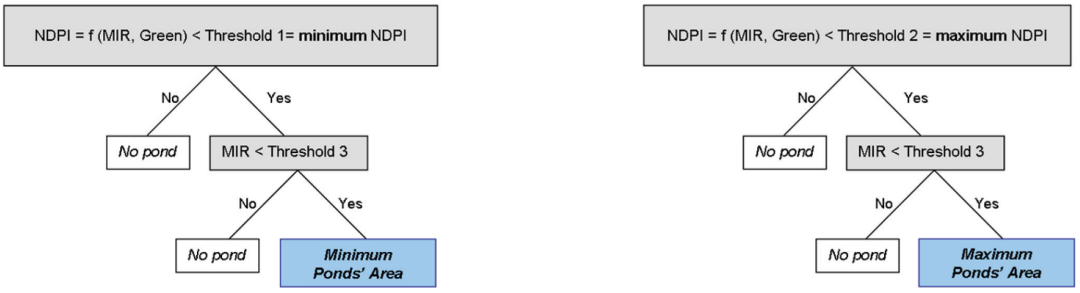

Fig. 1. Pond detection using two decision-tree conditional classifiers and photo-interpretation thresholds leading to identification of minimum (left) and maximum (right) pond areas. From these, the associated ZPOMs (with extremes) are constructed (see Fig. 3).

site). From the two ZPOMs, it is possible to calculate a mean ZPOM area (or ZPOMmean) and its uncertainties (σ, in %) as follows:

$$\text{ZPOMmean} = (\text{ZPOMmin} + \text{ZPOMmax})/2$$
$$\alpha = (((\text{ZPOMmax} - \text{ZPOMmin})/2)/\text{ZPOMmean})*100$$
$$\mathbf{Z} = \text{ZPOMmean} \pm \alpha$$

where ZPOMmin and ZPOMmax correspond to minimum and maximum ZPOMs' areas, respectively and **Z** signifies ZPOMs areas with uncertainties.

Results

In order to detail, and better understand, the relationships between rainfall events, ecozones, the distribution of ponds with associated rainfall variability (seasonal and inter-annual), the meridional transect was first displayed over the Senegalese precipitation climatology during the monsoon rainy season (1961-1990 averaged) and over the cumulated percentages of precipitation at the end of August 2003 (Fig. 2, left) and 2006 (Fig. 2, right). It is obvious that, in spite of a quasi-zonal distribution of isohyets from 300 mm to 100 mm over the transect (Fig. 2, left), this can be quite different when analyzed for individual years (Fig. 2, middle and right). For example, during 2003 (with large rainfall amounts recorded), the distribution was quasi-uniform over the whole transect. In contrast, during 2006, when precipitation was near to below the normal there was a definite difference between the northern part of the transect (approximately 50% of the area), where conditions were similar to that of 2003, and the southern part where they were almost normal (east of the transect) and below normal (80%) southwest of Linguere village. These differences should be expected to have different impacts on the pond distribution.

The false-color composite for 17 August 2006 and the associated ZPOMs extremes are displayed in Figure 3. The high-resolution images of the meridional transect allow comparisons between the four ecozones as identified by the Forestry Department of Senegal (DEFCCS) and are digitalized accordingly in Figure 3 (middle-left). Details of the latter (plus the hydrofossil riverbeds and cultivated areas) with their ZPOMs and the statistics are presented below.

The mid-range Senegal Valley River (12.6% of the transect area) lies north of the transect and is occupied by the Senegal River itself and the Doué branch which runs parallel to it. In this hydromorphic zone, two dams regulate the flooding of the mostly clayey soils during the rainy season, where "gonakiés trees" (*Acacia nilotica*) dominate, and where the "Oualo" region with richer soil allows agricultural activities such as producing maize, sorghum, sweet potatoes, cherry tomatoes, pumpkins, even late during the dry season. In the south, remnants of ancient cotton fields can be found on slightly elevated land. As can be expected, this is where the ZPOMs

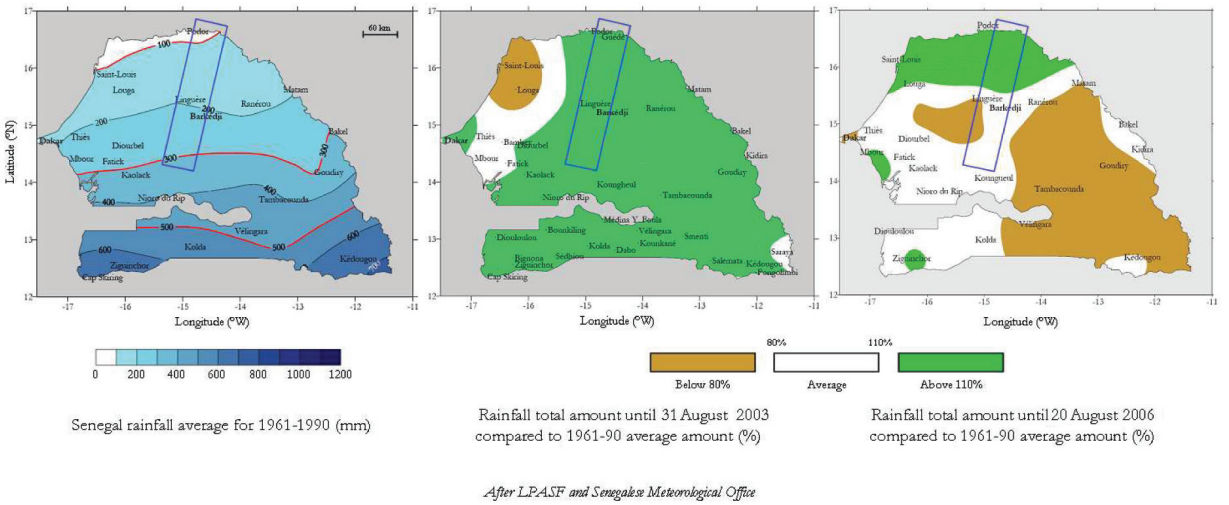

Fig. 2. The meridional transect in Senegal (slanted dark-blue rectangles) used in this study, super-imposed on Senegalese rainfall 30-year climatology (left panel), rainfall anomalies during 2003 (middle panel), and rainfall anomalies during 2006 (right panel). Averaged rainfall amount along isohyets are given in mm (left panel). Anomalies are in % and colour coded: light brown (below 80%), white (between 80% and 110%), and green (above 110%).

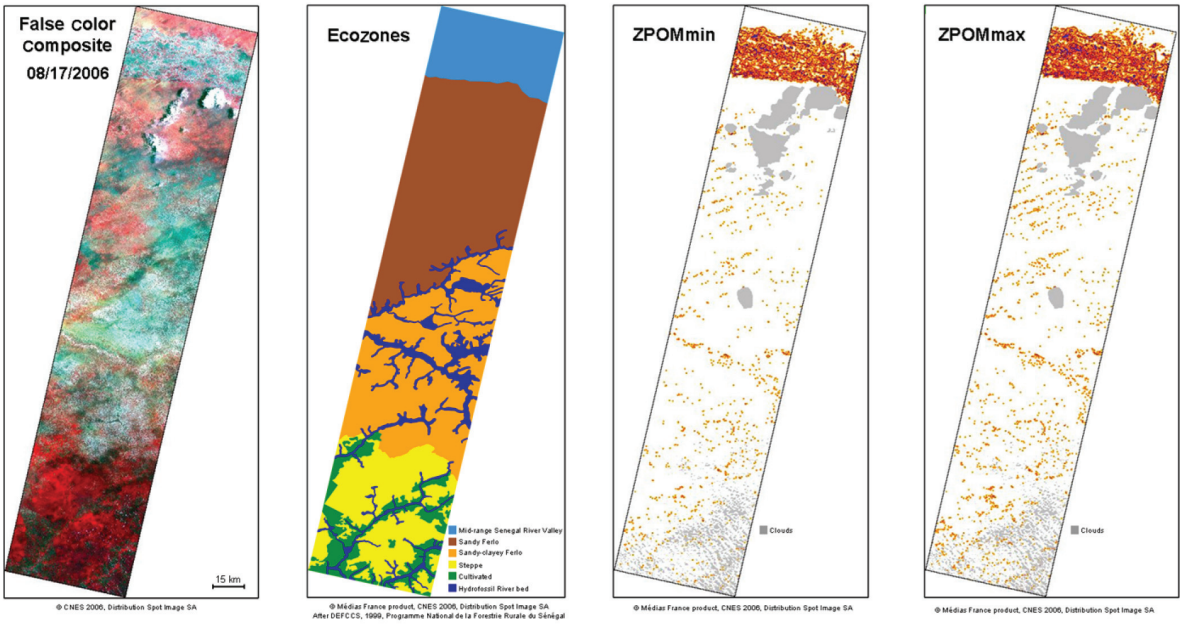

Fig. 3. Detailed analyses of the meridional transect with the following coordinates: 16° 50' 44" N and 14° 46' 34" W; 16° 43' 35" N and 14° 13' 48" W; 14° 18' 52" N and 15° 21' 53" W; 14° 11' 46" N and 14° 49' 31" W. The false-colour composite and data obtained from five SPOT-5 images and for 17 August 2006, are displayed at the left. In the middle-left panel the ecozones and hydrofossil valleys are digitized for precise statistics. The next two panels at the right are for the ZPOMs "extremes/uncertainties" in the vicinity of the pond during that time: ZPOMmin (middle right) and ZPOMmax (right). ZPOMs extensions in the text are expressed in hectares (ha), which correspond to a maximum distance of 500 m (i.e. mosquitoes' flying range) from the center of ponds. When small ponds are covered by one pixel, components of ZPOMs are circular in nature. The grey shading is due to clouds.

(extremes) occupy most of the terrain, i.e. 68% ± 1.8% during the rainy season. The total surface occupied by ponds attained 12,429 ha (or 6.4% of the ecozone) ± 9.8% as of 17 August 2006 and the total number of ponds was 4,623 ± 655 with a mean size of 2.7 ha.

The "sandy Ferlo" is found further south and in the upper-third of the transect (31.9%) where there are earth ridges and troughs with shrubbed savanna (shown in the figure as false-colour green strips oriented in a southwest-northeast fashion). This region is easily distinguished from the ferruginous zone of fossil ergs or ancient eroded dunes. The vegetation cover is degraded and floristically impoverished (mainly acacia) due to low average rainfall, human activity, and high concentrations of cattle around ponds and boreholes. This is particularly true since the breakdown of the Peul traditional pastoral system (Boutillier et al., 1962). The sandy, mobile soils have always been exposed to wind erosion, whilst the drought from the late 1960s has amplified the process. If we look at the ZPOMs (extremes) with a mean of 4.5% ± 1.2% of the "sandy Ferlo" (Fig. 3, middle-right and right) the same peculiar distribution is apparent with ponds aligned along troughs discussed above. In this ecozone the total surface of 366 ponds was 113 ha ± 25% with a mean size of 0.31 ha. The grey zones were not included in the statistical computation as they were due to clouds located there at the time when the images were retrieved.

The "sandy-clayey region" (Fig. 3, middle-left, near the middle of the transect) represents 33.7% of the transect area. It is bordered by a fossil river valley in the north which is oriented in the southwest-northeast direction and another fossil valley further south, oriented northwest-southeast in the Linguere/Barkedji region (the two fossil river beds account for 124,670 ha of the 400,440 ha of the sandy-clayey zone). The latter appears as an almost continuous and undulating white "thread" in the false-colour composite (Fig. 3, left). This is where most of the ponds align, particularly after intense rainy events and 362 ponds (out of 559) were detected here in 2006. The average pond size in the hydro-fossil riverbeds (0.4 ha) is twice that of the sandy-clayey zone. If we look at the ZPOMs (extremes) with a mean of 31,531 ha ± 14.8% or 6% of the ecozone (Fig. 3, middle-right and right), the distribution follows, as could be expected, that of the ponds along the main hydro-fossil riverbed aligned in the northwest-southeast direction. The pond density was almost six times larger in the riverbed than in the sandy-clayey zone. It should be noted that even if the sandy-clayey area was three times that of hydro-fossil riverbeds, the ponds and their contribution to ZPOMs were quite similar.

Finally, in the bottom third of the transect, the ecozone includes steppes (reddish false-colour) and cultivated areas of peanuts, mil, and string-beans fields (dark green false-colour) along the hydro-fossil riverbeds, which represents 21.8% of the transect area. This is the region where "séanes" (aquifers less than 5-10 m deep which re-surface between rains but which can be rapidly filled-up during intense rainfall). The hydro-fossil riverbed, in spite of its relatively small area (7.8% of the ecozone), includes 38.3% of the total number of ponds. In this ecozone, the ponds are not only equally distributed but displayed as 'cell-like' structures with a mean size of 0.18 ha. ZPOMs covering the steppes, hydro-fossil riverbed, and cultivated zones were 13,200 ha, 7,000 ha, and 4,500 ha, respectively. This is another case where ZPOM maps can be seen to be directly influenced by the spatial distribution of ponds. For example, pond density in the hydro-fossil riverbed was seven times higher than that of the steppes and ten times higher than in the cultivated zones.

The differences in the structural organizations of ponds, from linear southwest-northeast, linear northwest-southeast, cluster/cell-like are better represented in Figure 4. Here, the three different ecozones discussed above, with three different pond organizations (within 20 km x 20 km white squares; Fig. 4, left), are blown-up to highlight detailed patterns. They represent the "sandy Ferlo" to the north, the hydro-fossil riverbed near Barkedji (middle square), and the steppes/cultivat-

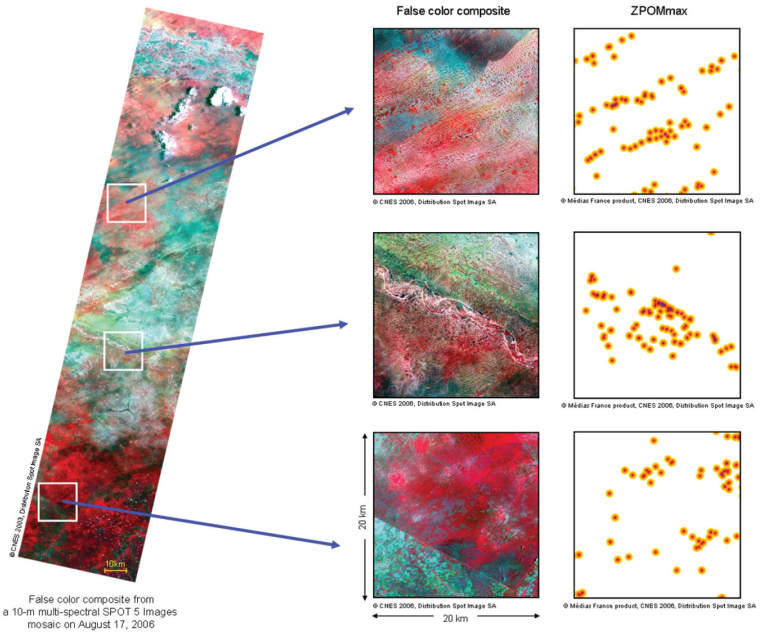

Fig. 4. Pond distribution and associated ZPOMmax are given for three ecozones within the white squares displayed over the false-colour composite (left panel). Blow-up of the three ecozones is thus given (middle panel, from top to bottom). The associated ZPOMmax and conspicuous patterns are displayed in the right panel (top to bottom). The middle figure in the right panel is in the vicinity of Barkedji used in Fig. 5.

ed areas to the south. The peculiar pond distributions (linear, clusters along the riverbed and cells-like) are well depicted within the three ZPOMmax (Fig. 4, right from top to bottom). As already mentioned when the fourth ecozone was discussed, the zone of particular RVF hazard (Fig. 4, bottom right) mainly covers the steppes (red false-colour) as compared to the cultivated areas (blue-green false-colour). On 17 August 2006, the ZPOMmax in the "sandy Ferlo", hydro-fossil riverbed (Barkedji village and site), and steppes/cultivated zones occupied 11.4%, 10.3%, and 8.4% of the zoomed areas, respectively.

Detailed ZPOMs inter-annual variability (with its minimum and maximum coverage) was obtained in the Barkedji zone (46 km x 43 km) at the end of August 2003 (a wet year) and 2006 (a near-normal year). ZPOMs extremes are displayed in Figure 5 along with the false-colour composites (Fig. 5, top) during these years (2003 in Fig. 5, left; 2006 in Fig. 5, right). Even if the previously identified northwest-southeast overall orientation of ponds along the hydro-fossil riverbed is made clearer for both 2003 and 2006, ZPOM differences between these two years are striking. During a normal year, rainfall triggers pond formation mostly within the hydro-fossil riverbed, while during an above-normal rainfall year, the density of temporary ponds increased evenly for almost all of the areas. Considering that the total rainfall amounts during the 2003 and 2006 rainy seasons until the time when the SPOT-5 images were obtained, it can be calculated that the 11 rainfalls for 2003 produced 212 mm (the image was taken three days after two rainfall events totalling 31 mm at Barkedji), while in 2006 the rainfall amounted to 143 mm emanating from nine events (the image was taken two days after a rainfall of 16 mm at Barkedji). The number of ponds was 7.3 times higher in 2003 than in 2006. The average size of the ponds was 1.08 ha in 2003 and 0.36 ha in 2006, i.e. ~3 times less. It is important to note that even if total pond surface area during 2006 (77

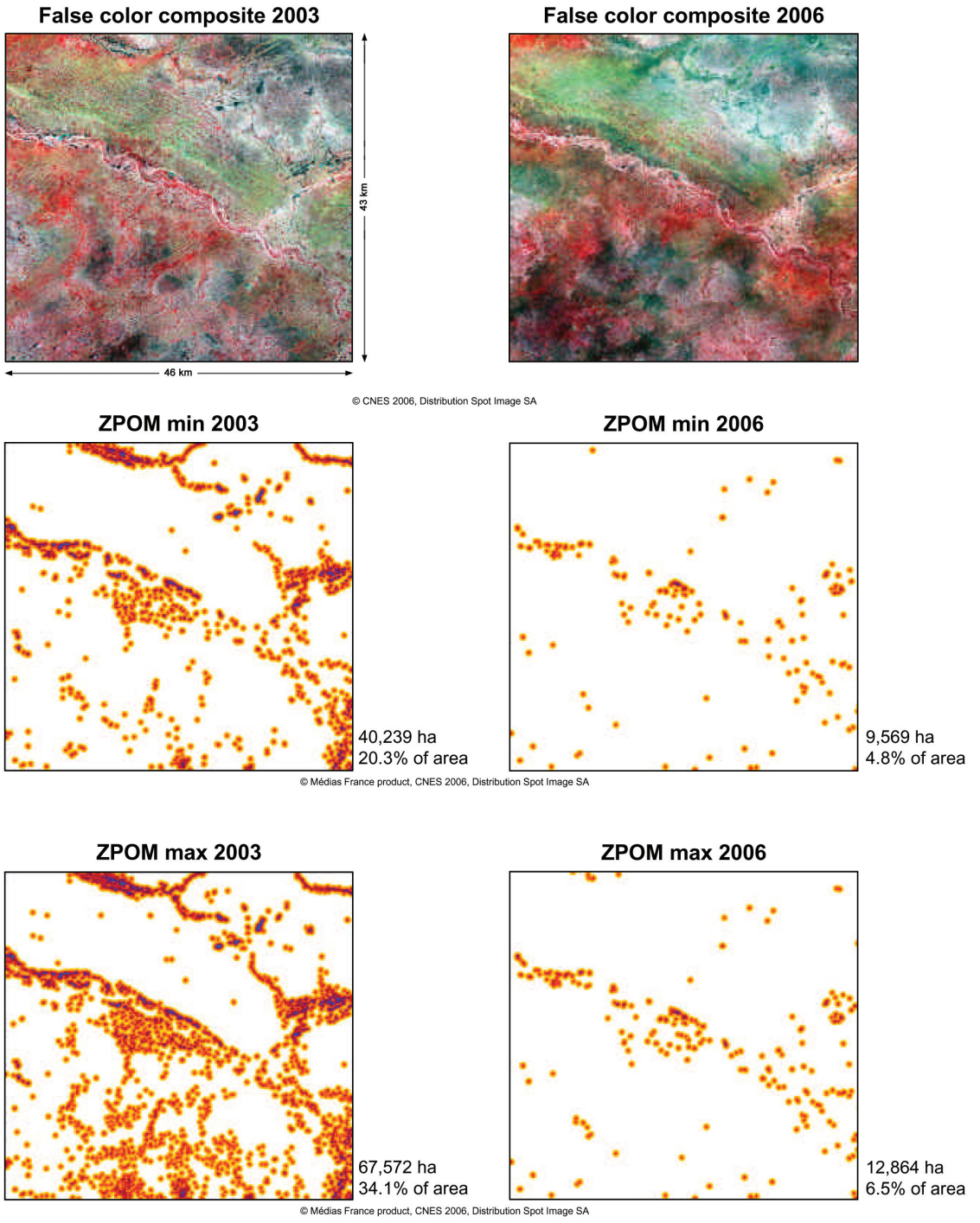

Fig. 5. Inter-annual variability of ZPOMs extremes for the 46 km x 43 km Barkedji scene: year 2003 in the left panel, year 2006 in the right panel. ZPOMs areas are expressed in ha and in % of the studied area.

ha) was 22 times less than during 2003 (1,700 ha), the corresponding ZPOMs surfaces were only five times less during 2006.

Discussion

The inter-annual variability of ponds and the associated ZPOMs show how strongly the environment can be modifield and how important the discrete variability of rainfall events is for the risk of RVF. It is recognized that the ZPOM presented here for the Senegalese transect is only a snapshot at the height of the rainy season (and for two climatically different years). In order to better understand vector dynamics and how it is linked to discrete rainfall and spatio-temporal variability of ponds, a dynamic ZPOM with entomological data (vector density and aggressiveness) would need to be produced. This type of information is important for strategic operations such as the positioning of livestock parks at night when the ruminants are in close contact with the vectors and thus reach a high risk of becoming virus reservoirs.

The spatial distribution of ponds associated with different ecozones, substructure of aquifers, and spatio-temporal distribution of rainfall events are all very important for ZPOM mapping. Extreme rainfall events (>20 mm of cumulated rain from squall-lines) rapidly increase the number and pond areas. These events modify the environment in favour of mosquito larval production and could trigger and enhance mosquito reproduction for one to two weeks after a discrete rainy event as proposed by Mondet et al. (2005b) and Ndiaye et al. (2006). Based on pond location and remote-sensing composite analysis, ZPOMs (i.e. extremes from uncertainties linked to RS image processing) could for the first time be constructed for large areas such as the meridional transect in the Sahelian region of Senegal.

The precise location of ponds (down to a size of 0.1 ha), common when rainfall is at its maximum, is a prerequisite for accurate mapping of ZPOMs. This was accomplished by using high-resolution RS data obtained during the height of the rainy season. It was found that a total pond area of 12,817 ha ± 10%, i.e. about 0.8% of the meridional transect area, corresponded to an average ZPOM which is 17 times larger, i.e. 212,813 ha ± 10% (or about 14% of the transect). Thus, ponds and the associated ZPOMs inter-annual variability can be highlighted by comparing their statistics (numbers and coverage). This was done in the vicinity of Barkedji (a sandy-clayey ecozone, crossed by an important hydrofossil river bed) for two different years: the very humid year of 2003, and the near/below normal rainfall year of 2006. It was shown that pond areas at the end of August 2003 were already approximately 22 times larger than at the end of August 2006 when it was about five times larger, whilst the corresponding uncertainties on ZPOMs extensions were 25.4% and 14.7%, respectively. Knowledge of ZPOMs variability has great implication for strategic prevention of cattle exposure to RVF vectors, human activities and mitigation of socio-economical impacts. Preliminary results indicate that during the normal rainfall year of 2003, about 50 to 80% of all parks in the Barkedji area were within the associated ZPOM. For example, one park of five is located one day of four in zones highly exposed to *Ae. vexans*. Taking rainfall amount and frequency into account, the resulting overall number and size of ponds can be foreseen and thus the risks of animals for being in contact with vectors, quantified. In order to quantify the true risks for animals being in contact with the RVF vectors and increase the accuracy of predictions, vector aggressiveness should be added to the ZPOMs data by super-imposing this information to the localized, geo-referenced parks.

Combining a multi-disciplinary and integrated approach involving rainfall data (seasonal forecasts and near real-time observations), ponds and differences in ZPOMs as a function of ecozones, biological data such as vector aggressiveness, virus transmission and pastoralism, should make it possible to evaluate dynamical RVF risks. The snap-shot results presented here represent a first step for the above

procedure. Release of such operational products will have great implication for strategic prevention of cattle exposure to RVF vectors and mitigation of epidemics. This conceptual approach is meant to be included rapidly within RVF early-warning systems (RVFEWS) particularly important in climate change context (see also Ceccato et al., 2005) and adapted to other vector-borne diseases within the "Sahelian window" and elsewhere.

Acknowledgements

We thank Dr. Antonio Güell, Head of the "Applications and Valorisations" office at CNES, for funding this study, and the CNES/ISIS program which permitted access to high-spatial resolution SPOT-5 images and data. Yves M. Tourre thanks particularly Drs. Mike Purdy, Jean-Claude André, and Philippe Dandin, Director of LDEO, CERFACS and DCLIM/METEO-France, respectively, for their unconditional support and the Geospatial Health editorial team for its excellent remarks and efficiency. This research is a part of the AMMA Health Application Work Package: WP 3.4. It is also a LDEO contribution # 7207.

References

Aranyossy JF, Faye A, Møller KN, Sarr M, Emsellem Y, 2006. Input of chemical and isotopic studies in the elaboration of the new conceptual flow model of the Maastrichtien aquifer system in Senegal. International Symposium on Aquifers Systems Management Dijon, France, p. 75.

Bâ Y, Diallo D, Fadel Kebe CM, Dia I, Diallo M, 2005. Aspects of bio ecology of two Rift Valley fever virus vectors in Senegal (West Africa): *Aedes vexans* and *Culex poicilipes* (Diptera: Culicidae). J Med Entomol 42, 739-750.

Boutillier J-L, Cantrelle P, Caussé J, Laurent C, N'Doye T, 1962. La moyenne vallée du Sénégal. I. N. S. E. E Service de la Coopération. Presses Universitaires de France, 368 pp.

Ceccato P, Connor SJ, Jeanne I, Thomson MC, 2005. Application of geographical information systems and remote sensing technologies for assessing and monitoring malaria risk. Parassitologia 47, 81-96.

Chevalier V, Lancelot R, Thiongane Y, Sall B, Diaïté A, Mondet B, 2005. Rift Valley fever in small ruminants, Senegal, 2003. Emerg Infect Dis 11, 1693-1700.

CNES, 2008. Method for tele-epidemiology (Méthode pour la télé-épidémiologie). Patent pending.

Diallo M, Nabeth P, Bâ K, Sall AA, Bâ Y, Mondo M, Girault L, Abdalahi MO, Mathiot C, 2005. Mosquitoe vectors of the 1998-1999 outbreak of Rift Valley fever and other arboviruses (Bagaza, Sanar, Wesselsbron and West Nile) in Mauritania and Senegal. Med Vet Entomol 19, 119-126.

Gao BC, 1996. NDWI - a normalized difference water index for remote sensing of vegetation liquid water from space. Remote Sens Environ 58, 257-266.

Fontenille D, Traoré-Lamizana M, Diallo M, Thonnon J, Digoutte J-P, Zeller HG, 1998. New vectors of Rift Valley fever in West Africa. Emerg Infect Dis 4, 289-293.

Lacaux J-P, Tourre YM, Vignolles C, Ndione J-A, Lafaye M, 2007. Classification of ponds from high-spatial resolution remote sensing: application to Rift Valley fever epidemics in Senegal. Remote Sens Environ 106, 66-74.

Linthicum KJ, Anyamba A, Tucker CJ, Kelley PW, Myers MF, Peters CJ, 1999. Climate and satellite indicators to forecast Rift Valley epidemics in Kenya. Science 285, 397-400.

McFeeters SK, 1996. The use of the normalized difference water index (NDWI) in the delineation of open water features. Int J Remote Sens 17, 1425-1432.

Meegan JM, Bailey CL, 1988. Rift Valley fever. In: The arboviruses epidemiology and ecology, Vol. IV. Monath TP (ed). CRC Press, Inc., Boca Raton, FL, USA, pp. 51-76.

Mondet B, Diaïté A, Fall AG, Chevalier V, 2005a. Relations entre la pluviométrie et le risque de transmission virale par les moustiques: cas du virus de la Rift Valley fever (RVF) dans le Ferlo (Sénégal). Environ Ris Santé 4, 125-129.

Mondet B, Diaïté A, Ndione J-A, Fall AG, Chevalier V, Lancelot R, Ndiaye M, Ponçon N, 2005b. Rainfall patterns and population dynamics of *Aedes (Aedimorphus) vexans arabiensis*, Patton 1905 (Diptera: Culicidae), a potential vector of Rift Valley fever virus in Senegal. J Vector Ecol 30, 102-106.

Ndiaye PI, Bicout D, Mondet B, Sabatier P, 2006. Rainfall triggered dynamics of *Aedes* mosquito aggressiveness. J Theoret Biol 243, 222-229.

Ndione J-A, Besancenot J-P, Lacaux J-P, Sabatier P, 2003. Environnement et épidémiologie de la fièvre de la vallée du Rift (FVR) dans le bassin inférieur du fleuve Sénégal. Environ Ris Santé 2, 1-7.

Paaijmans KP, Takken W, Githeko AK, Jacobs AFG, 2008. The effect of water turbidity on the near-surface water temperature of larval habitats of the malaria mosquito *Anopheles gambiae*. Int J Biometeorol, doi: 10.1007/s00484-008-0167-2.

Pinzon JE, Wilson JM, Tucker CJ, 2005. Climate-based health monitoring systems for eco-climatic conditions associated with infectious diseases. Bull Soc Pathol Exot 98, 239-243.

Porphyre T, Bicout DJ, Sabatier P, 2005. Modelling the abundance of mosquito vectors *versus* flooding dynamics. Ecol Modell 183, 173-181.

Thomson MC, Doblas-Reyes FJ, Mason SJ, Hagedorn R, Connor SJ, Phindela T, Morse AP, Palmer T, 2006. Malaria early warnings based on seasonal climate forecasts from multi-model ensembles. Nature 439, 576-579.

Wilson ML, Chapman LE, Hall DB, Dykstra EA, Ba K, Zeller HG, Traore-Lamizana M, Hervy J-P, Linthicum KJ, Peters CJ, 1994. Rift Valley fever in rural northern Senegal: human risk factors and potential vectors. Am J Trop Med Hyg 50, 663-675.

Xu H, 2006. Modification of the normalised difference water index (NDWI) to enhance open water features in remotely sensed imagery. Int J Remote Sens 27, 3025-3033.

Yi Y, Yang D, Chen D, Huang J, 2007. Retrieving crop physiological parameters and assessing water deficiency using MODIS data during the winter wheat growing period. Canad J Remote Sens 33, 189-202.